Graphitic carbon nitride as a photocatalyst for decarboxylative C(sp^2)–C(sp^3) couplings *via* nickel catalysis

Florian Lukas,[1,†] *Michael T. Findlay,*[1,†] *Méritxell Fillols,*[1] *Johanna Templ,*[1,2] *Elia Savino,*[1] *Benjamin Martin,*[3] *Simon Allmendinger,*[3] *Markus Furegati,*[3] *and Timothy Noël* [1,*]

[1] Flow Chemistry Group, Van 't Hoff Institute for Molecular Sciences (HIMS), University of Amsterdam, Science Park 904, 1098 XH Amsterdam, The Netherlands.

[2] Institute of Applied Synthetic Chemistry, TU Wien, Getreidemarkt 9/E163, 1060 Vienna (Austria).

[3] Novartis Pharma AG, Fabrikstrasse, 4002 Basel, Switzerland.

[†] These authors contributed equally to this work.

* *Email:* t.noel@uva.nl

Keywords: Graphitic carbon nitride • Decarboxylation • Heterogeneous photocatalysis • Metallaphotoredox • Nickel

Graphical abstract

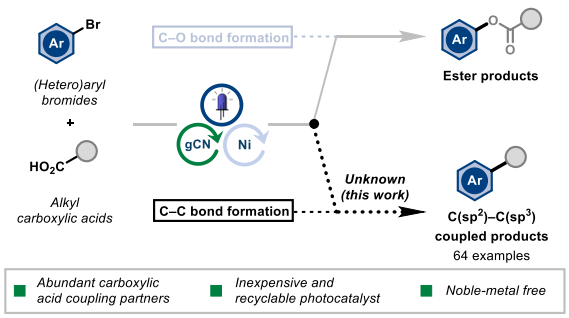

ABSTRACT

The development of robust and reliable methods for the construction of C(sp^2)–C(sp^3) bonds is vital for accessing an increased array of structurally diverse scaffolds in drug discovery and development campaigns. While significant advances towards this goal have been achieved using metallaphotoredox chemistry, many of these methods utilise photocatalysts based on precious-metals due to their efficient redox processes and tuneable properties. However, due to the cost, scarcity, and toxicity of these metals, the search for suitable replacements should be a priority. Here, we show the use of commercially available heterogeneous semiconductor graphitic carbon nitride (g-C_3N_4) as a

photocatalyst, combined with nickel catalysis, for the cross-coupling between aryl halide and carboxylic acid coupling partners. g-C_3N_4 has been shown to engage in single-electron-transfer (SET) and energy-transfer (ET) processes for the formation of C–X bonds, and in this manuscript we overcome previous limitations to furnish C–C over C–O bonds using carboxylic acids. A broad scope of both aryl halides and carboxylic acids is presented, and recycling of the photocatalyst demonstrated. The mechanism of the reaction is also investigated.

MAIN TEXT

Introduction

The selective transition-metal catalysed cross-coupling of two fragments to form new C–C bonds has become an indispensable tool for the modern synthetic chemist. Despite the relatively high cost of palladium, traditional methods have favoured its use in cross-coupling due to its high catalytic activity, substrate compatibility, and the broad range of transformations that are possible.[1] More recently, however, in the search for catalytic systems that rely on earth-abundant metals, nickel has emerged as a valuable alternative to palladium for cross-coupling.[2,3] In addition to its lower cost and greater abundance, nickel possesses a different reactivity profile to palladium: displaying a reduced propensity of Ni-alkyl intermediates to undergo β–hydride elimination, and possessing a broader array of accessible oxidation states (0, +1, +2, +3, +4), meaning that both two- and one-electron redox processes are possible.[4–6] These properties mean that nickel is now often the metal of choice for metallaphotoredox C(sp^2)–C(sp^3) bond formation, with seminal examples being reported in 2014 by both Molander, using potassium trifluoroborate salts, and MacMillan and Doyle, using carboxylic acids as radical precursors, along with aryl halides, to form new bonds using a dual nickel-iridium catalysed system (Scheme **1A**).[7,8] Since then, a wide variety of radical precursors as coupling partners has been reported, expanding the possible synthetic disconnections available for synthetic chemists.[8–17]

Despite the use of an earth abundant base metal catalyst, metallaphotoredox methods with nickel still often rely on the use of precious-metal iridium-based photocatalysts.[18] The high cost and relative scarcity of iridium often becomes an overriding factor in the use of these procedures, which becomes increasingly problematic as scale increases. As such, a substitution for cheaper, noble-metal free, and recyclable catalysts would open up use of the concept for broader exploitation. Heterogeneous semiconductors have garnered interest in the field of photocatalysis as a result of their relatively cheap cost, robust nature, and the ability to be filtered and recovered owing to their insoluble nature.[19,20] Suitable semiconductor photocatalysts possess a band gap that can be excited with light from the UV or visible light regions in order to participate in single electron transfer (SET) redox processes, which can be modified by doping of these photocatalysts with additional elements. Recent

reports have shown that metal-free graphitic carbon nitrides (gCNs) are effective photocatalysts in organic synthesis, and are capable of a growing number of transformations.[21–25] Indeed, it has been shown that with carboxylic acid coupling partners, efficient oxidatively induced radical decarboxylation can take place to generate alkyl radical intermediates. These radicals can then react with a range coupling partners to form C–H,[26] C–C,[26–28] C–N,[28] and C–O[29] bonds (Scheme **1B**).

Whilst direct C–C bond formation *via* a dual gCN/nickel manifold was reported by the König group in 2020 using benzylic and allylic potassium trifluoroborate salts as radical precursors,[30] attempts to use carboxylic acids directly in combination with g-CN photocatalysts have been hampered by the propensity of nickel-carboxylate complexes to undergo energy-transfer-mediated ester-formation, as opposed of the desired single electron transfer mediated decarboxylation and subsequent transition-metal coupling (Scheme **1C**).[31,32] The carboxylic acid functional group is highly prevalent in organic molecules, has broad commercial availability, low toxicity, and good benchtop stability, and as such, is a highly desirable source of alkyl radicals for cross-coupling.[33–35] In revisiting this concept we have managed to overcome earlier roadblocks and herein we report the application of g-CN in dual nickel/photocatalysis for decarboxylative C(sp^2)-C(sp^3) bond formation.

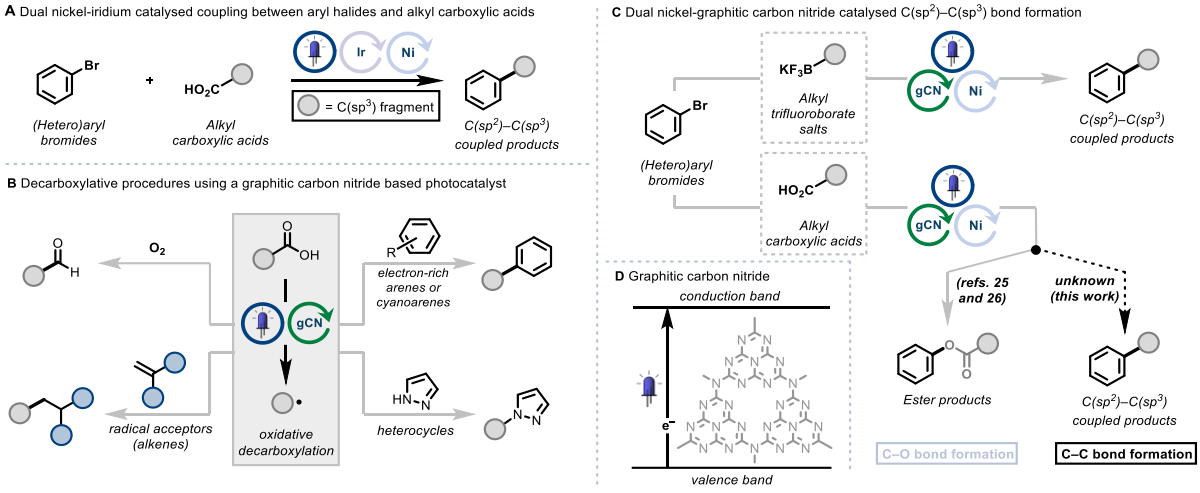

Scheme 1. A. Metallophotoredox protocol developed by the MacMillan group for C(sp^2)-C(sp^3) coupling, B. Decarboxylative bond formation catalysed by graphitic carbon nitride based photocatalyst, C. Dual graphitic-carbon nitride/nickel systems with alkyl trifluoroborate salts and carboxylic acids, D. Graphitic carbon nitride structure.

Results and Discussion

We started our investigation by using methyl 4-bromobenzoate (**1**) and 4-biphenyl acetic acid (**2**) with commercial gCN photocatalyst, $NiBr_2$.glyme, and dtbbpy, with irradiation with a 390 nm Kessil lamp for 24 h, in order to achieve decarboxylative C–C bond formation. Initial results led us only to obtaining exclusive C–O (ester or phenol) bond formation or low reactivity in place of the desired C–C coupled product. Pleasingly, we found that using MeCN as solvent generated the desired product (**3**) in a moderate

32% yield, however, this was accompanied by the formation of unwanted ester, phenol and protodehalogenated side products. The presence of both the reduced carboxylic acid and its dimer in large quantities suggested that oxidation of the carboxylic acid by the photocatalyst and subsequent decarboxylation were taking place but the radical intermediate was participating in undesired side-reactions before combination with the nickel complex. We found that the heterogeneous nature of the reaction mixture led to some inconsistencies in mixing efficiency, and changing our reaction setup to ensure excellent stirring (see supporting information for details) led to an increased and reproducible reaction yield. Further systematic screening of our reaction parameters allowed us to identify optimal reaction conditions: using 1.5 equivalents of both the acid and base, 5 mol % of nickel with a 4,4'-diphenyl substituted bipyridyl ligand (dPh-bpy), and 1.0 equivalent of phthalimide additive, as described by MacMillan,[36] led to isolation of **3** in a high 89% isolated yield (Table 1, Entry 1). DMF or DMSO as solvent led to no or low yields of the target product **3** (Table 1, Entry 2), and using K_2CO_3, $CsHCO_3$, or BTMG as base generated product **3** in lower yields in comparison to Cs_2CO_3 (Table 1, Entry 3). When the reaction was performed with 1:1:1 stoichiometry between aryl halide, acid and base, a product yield of 70% was still observed, in conditions that would be preferential when using valuable carboxylic acids. 4-methyl iodobenzoate performed similarly to the aryl bromides, albeit giving a lower yield of 63%, however, switching to 4-methylchlorobenzoate significantly reduced the formation of **3**, generating 25% after 24 h. Performing the reaction with no phthalimide additive saw a reduction in yield to 45% (Table 1, Entry 6), and additional control experiments showed that in the absence of light, nickel or ligand, or base, no reactivity was observed, confirming the necessity of these components of the reaction.

Table 1. Reaction optimization.

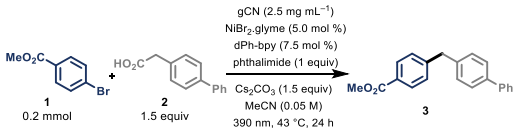

Entry	Variation	3 (%)
1	None	92 (89)
2	DMF/DMSO as solvent	> 5%
3	K_2CO_3/$CsHCO_3$/BTMG as base	60/69/52
4	1:1 stoichiometry	70
5	4-methyl iodobenzoate	63
6	4-methyl chlorobenzoate	25
7	No phthalimide	45
8	No photocatalyst	0
9	No nickel	0
10	No light	0

Yields determined by NMR analysis of the crude reaction mixture using trichloroethene as an external standard. Values in parentheses are yields of the isolated compound.

With our optimised conditions in hand, we investigated the scope of the carboxylic acid coupling partner (Scheme **2**). We found that a wide range of benzylic carboxylic acids bearing either electron-donating or halogen substituents in the *para*-position were amenable to the reaction conditions, forming diarylmethane derivate products **4**-**7** in good to excellent yields. In comparison, acids bearing electron-withdrawing groups in the *para*-position were less reactive (**8**-**10**), although increasing the acid and base loading from 1.5 equiv to 3.0 equiv for products **9** and **10** increased the yield, generating 61% and 42% product yields respectively. Phenylacetic acid, bearing no substitution on the phenyl ring, generated product **11** in a 64% yield, and the addition of a fluorine atom in the α-position to the acid group had little effect on the yield, delivering product **12** in a 53% yield. In addition to phenyl substituted acetic acid derivatives, naphthalene (**14**, 81%), furan (**15**, 69%) and thiophene cores (**16**, 71%) were tolerated under the reaction conditions, generating the product in good yields. Indomethacin, a nonsteroidal anti-inflammatory drug containing a carboxylic acid group and a polysubsituted indole core, was able to be functionalised, generating product **17** in a 51% yield. Unfortunately, acids bearing substitution at the *ortho*-position of the phenyl ring, along with secondary and tertiary 2-phenylacetic acids, did not yield the desired products when subjected to the standard reaction conditions (for examples of incompatible coupling partners, see supporting information). We were also able to scale up this procedure starting from 10 mmol of aryl halide, resulting in 77% of product **3** with minimum alteration of the reaction setup.

Shifting our focus onto α-oxygen carboxylic acids, we found that primary (**18** and **19**), acyclic secondary (**20**), and cyclic substrates with various ring sizes (**21**-**23**) were all transformed selectively into the C–C coupled products, in addition to an α-sulphur carboxylic acid providing product **29**. Cheap and abundant α-amino acids also proved to be excellent coupling partners, transforming protected glycine, alanine, proline, tryptophan, and tyrosine, in addition to two unnatural amino acids, into the corresponding C–C coupled products (**24**-**32**). A glycine-alanine dipeptide and a glycine-leucine-threonine tripeptide were also functionalised, demonstrating the extension of the methodology beyond single amino acids (**33** and **34**). Applying the methodology to substrates bearing no stabilising group *alpha*- to the carboxylic acid proved more challenging and in general lower yields were seen under the standard conditions. However, using an increasing amount of acid substrate and base and extended reaction times led to appreciable yields of the desired coupling products. Primary acids, and cyclic secondary acids containing an oxygen or nitrogen heteroatom worked well (**35**-**37**). Interestingly, it was possible to transform the acid side chain of both aspartic acid (**38**) and glutamic acid (**39**), allowing access to derivatives of phenylalanine and homophenylalanine in a single step, potentially allowing the synthesis of a library of a diverse range of unnatural amino acid derivatives using our methodology. Finally, with the use of acetic acid as a cheap, non-toxic methylating reagent, it was possible to generate methylated product **40** in 23% yield. This route avoids the use of highly electrophilic methylating agents, and could be utilised for the late-stage functionalisation of target molecules in drug discovery campaigns.

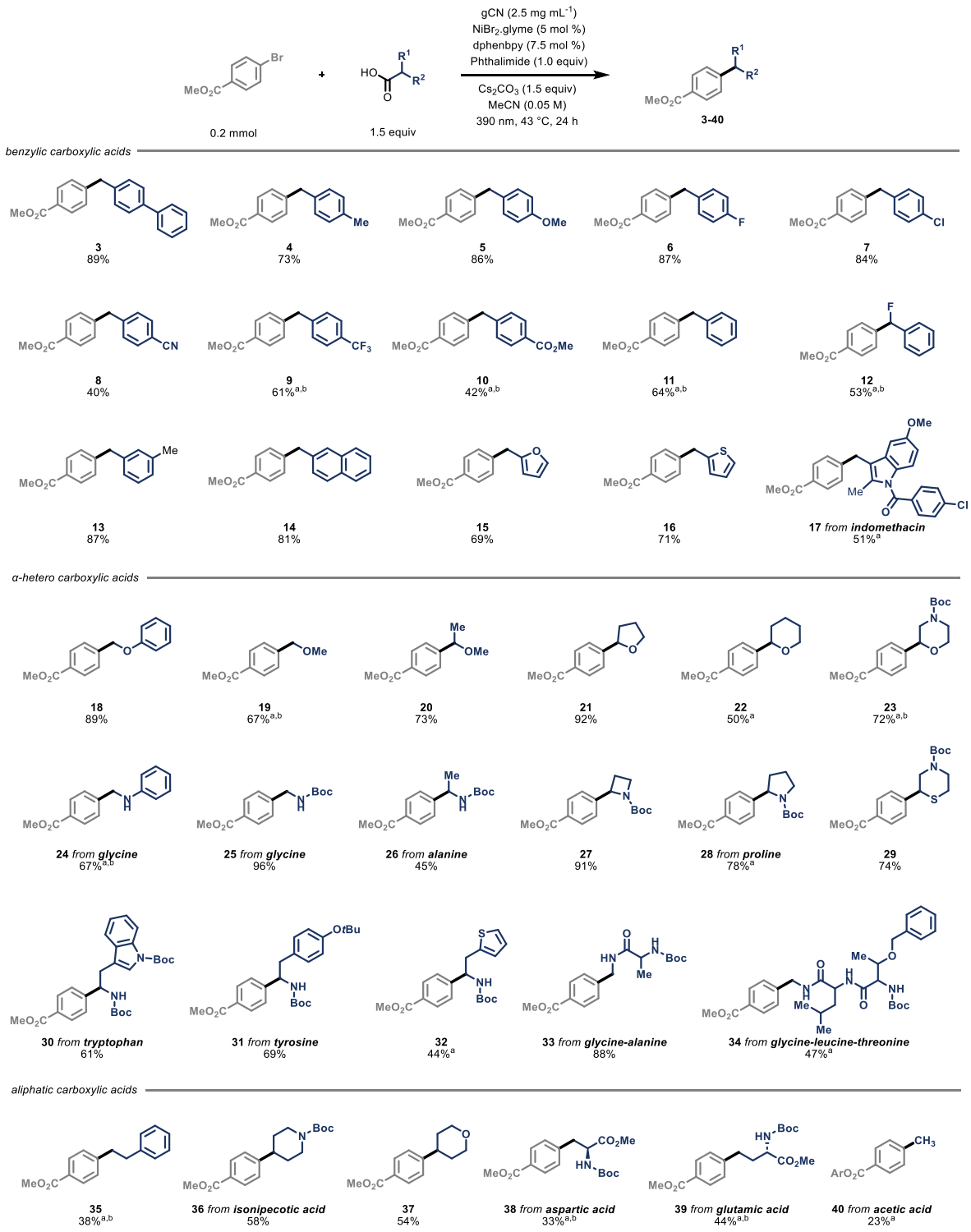

Scheme 2. Scope of carboxylic acid coupling partners. All yields are of isolated compounds. Ar = 4-methylbenzene. (a) Reaction time: 48 h, (b) **Carboxylic acid** (3 equiv) and **Cs_2CO_3** (3 equiv).

Turning our attention to the aryl halide coupling partner, we found that a wide range of substituents in the position *para* to the halide were tolerated in our reaction system (**3**, **41-47**). In addition to electron-withdrawing trifluoromethyl (CF_3) (**42**) and cyano (CN) (**43**) substituents, 1-bromo-4-chlorobenzene reacted exclusively through the carbon-bromide bond (**41**), with the carbon-chloride bond remaining

untouched and suitable for further downstream functionalisation. Aryl halides bearing more sensitive functional groups were also viable coupling partners, with examples containing a sulfonamide, aldehyde, and benzylic alcohol remaining unreacted during the transformation, giving products **45**, **46** and **47** in synthetically useful yields. While substitution in the *meta*-position of aryl halides had no effect on the reaction yield, with products **48** and **49** being formed in high yields, *ortho*-substitution proved deleterious, generating products only in very low yields or displaying no reactivity (see supporting information for details on incompatible aryl halide coupling partners). Exploring heterocyclic scaffolds, which are highly prevalent in APIs, we found that 2-, 3- and 4-bromo-pyridine isomers were suitable coupling partners, with the position of the bromide substituent relative to the pyridine nitrogen resulting in little difference to the final product yield (**50**-**54**). 2-Bromo-6-chloropyridine also reacted exclusively at the carbon–bromide bond, with the chloride substituent remaining unfunctionalised under the reaction conditions (**53**). This reaction was not limited to pyridines, with $–CF_3$ substituted pyrimidine also generating product **55** in a 55% yield. In addition to 6-membered nitrogen heterocycles, fused nitrogen heterocycles containing quinoline, boc-protected indole, imidazopyridine, and *N*-Me-benzotriazole moieties were tolerated by the reaction conditions (**56**-**59**), demonstrating the utility of this method for synthesis of complex bioactive targets. 1,4-dichloropyrazine reacted efficiently at the carbon–chlorine bond, to deliver product **60** in a 65% yield, without any overreaction being observed. Further products containing the benzothiopene (**61**) and phthalide (**62**) bicyclic structures were formed smoothly from their corresponding aryl bromides in high yields. To further show the synthetic applications of the new method, we synthesized in a single step the thiazole building block **63** (66%), which is commonly encountered as the C-Terminus of a number of peptides found in marine cyanobacteria, most notably biseokeaniamides A–C.[37] Notably, synthesis of this compound required previously a 3-step procedure. Finally, we discovered that the protocol is not only effective towards arylation, but also vinylation, as shown by transformation of a *β*-bromo-styrene to product **64** under the same reaction conditions (68% isolated yield).

Furthermore, we were able to deliver **65**, which after facile bromination to **66** can be easily developed into aromatase inhibitor *vorozole* by a literature described procedure (Scheme **3B**).[38] To conclude we applied conditions reported by Xu et al. to product **44**, enabling the synthesis of derivatives of antifungal drug bifonazole (Scheme **3C** - **67, 68**).[39]

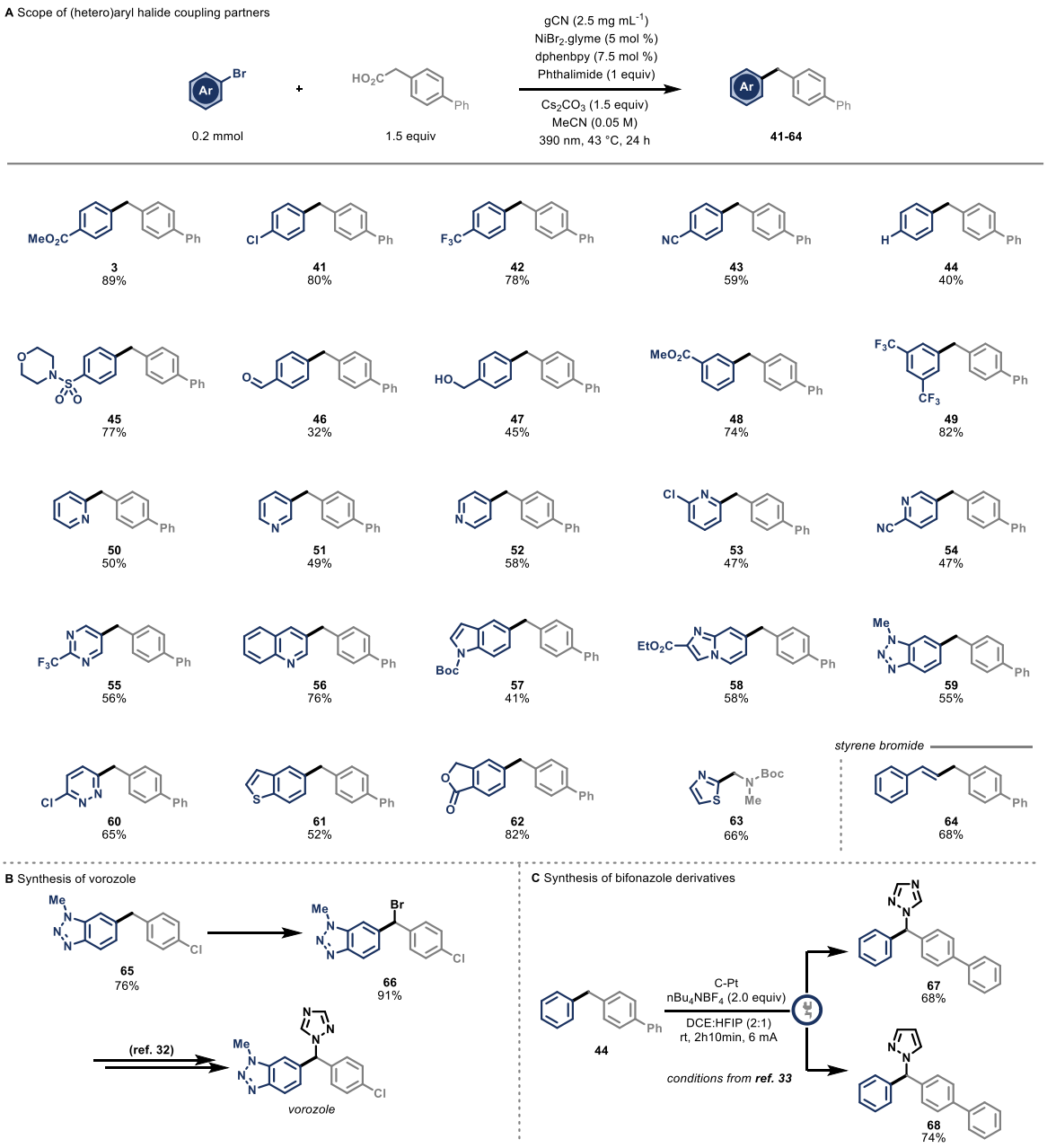

Scheme 3. Scope of aryl halide coupling partner. All yields are of isolated compounds.

In order to test the robust and reproducible nature of using graphitic carbon nitride as photocatalyst, we performed the model reaction shown with different commercial suppliers of gCN (Scheme **4A**). Pleasingly, while a difference in reaction rates was observed (see supporting information), consistent product yield after 24 h was observed when using 3 different commercial suppliers, suggesting that this reactivity is not limited to a single batch of photocatalyst.[40] Next, to demonstrate its recyclability, we set out to recover and reuse the graphitic carbon nitride from the reaction mixture in subsequent reactions. Photocatalysts based on homogeneous transition-metal complexes are susceptible to degradation over time, and their separation from the reaction mixture after use can be challenging,[41] adding difficulty to the recycling process. In contrast, the robust, insoluble and heterogeneous nature of graphitic carbon nitride

allows it to be recovered unchanged using simple laboratory techniques to filter out solids. In our case, by using centrifugation followed by solid washing steps, we demonstrated that the photocatalyst could be used under the same reaction conditions 5 times without loss of product yield after 24 h. X-ray diffraction and FT-IR measurements taken before and after the reaction indicated that no clear structural change had taken place.

We then decided to evaluate the environmental impact of our procedure *via* comparison with an analogous iridium-catalysed process. A 30 mmol scale-up of the nickel/iridium catalysed procedure initially reported by MacMillan was reported by chemists from Bayer AG Pharmaceuticals in 2020, using an immersion-well batch-reactor.[42] We calculated the Total Carbon Release (TCR), a metric developed by Novartis to assess the environmental impact of chemical processes, for the two procedures, providing a breakdown of the contribution from solvent, reagents, and photocatalyst (Scheme **4B**).[43,44] Whilst the TCR ($kgCO_2eq/kg$) we calculated from solvent and reagents was approximately equal for both procedures, the contribution from the photocatalyst differs greatly. In the case of iridium, the contribution is 491 $kgCO_2eq/kg$, accounting for over 50% of the TCR of the entire process. In contrast, the contribution from gCN accounts for <1% of the TCR of the synthesis, and results in a value of <50% of that of the iridium-based process.

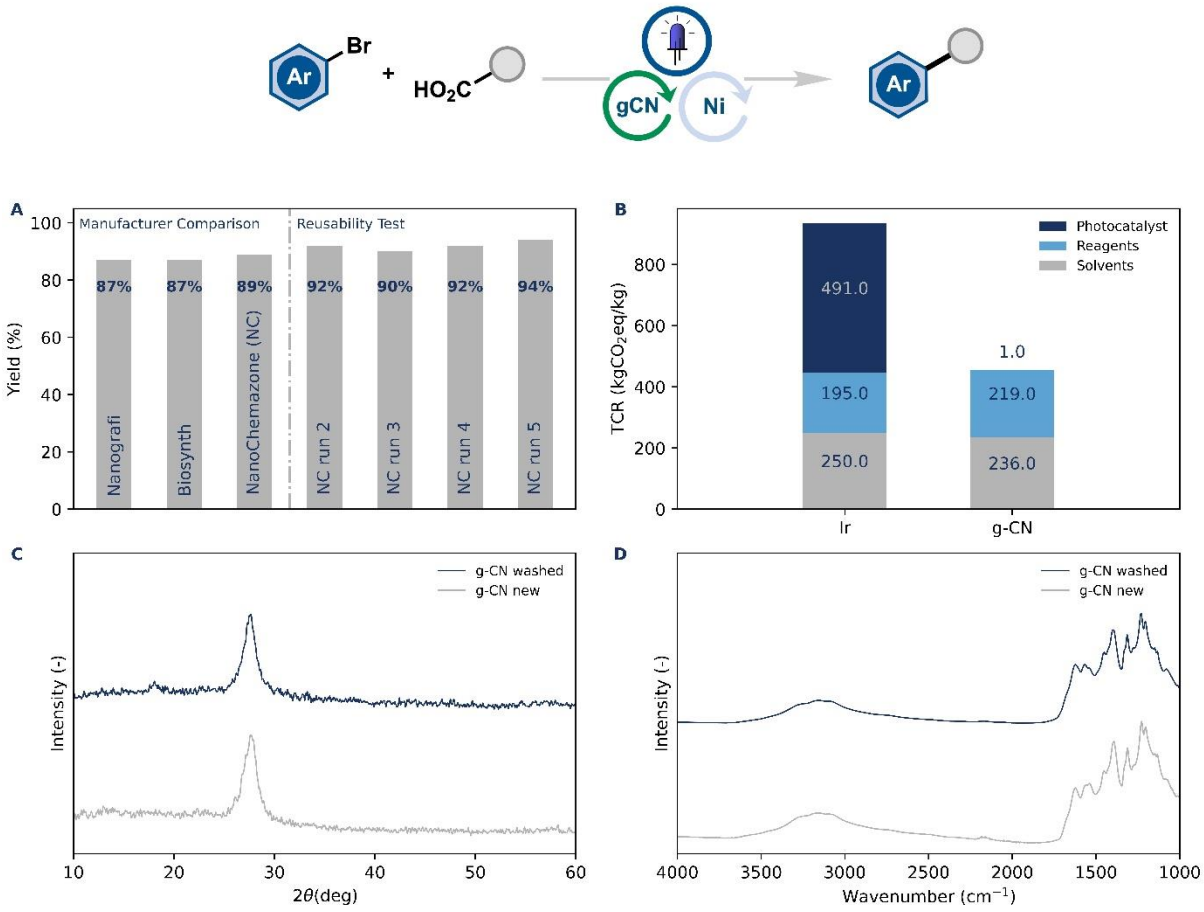

Scheme 4. (A) Yields of reactions performed with different suppliers of gCN, and yields of reactions performed with continuous recycling of gCN, (B) Total Carbon Release (TCR) calculated for iridium-based and gCN-based decarboxylative cross coupling, (C) XRD spectra of new and washed gCN, (D) FTIR spectra of new and washed gCN.

Finally, we examined some aspects of the reaction mechanism (Scheme **5**). While the exact mechanism of nickel-catalysed cross-couplings is complex, we propose a plausible mechanistic route based on earlier works in the field (Scheme **5D**). For the gCN, upon irradiation with 390 nm light an electron is promoted from the valence band to the conduction band, forming an electron-hole pair. The gCN then facilitates oxidation of the carboxylate *via* a reductive quenching cycle to form a carboxylate radical, which rapidly undergoes decarboxylation to form a carbon-centred radical. Concurrently, the aryl bromide oxidatively adds to the Ni(0) complex **I**, delivering Ni(II)-aryl complex **II**. After addition of the acid derived radical to form Ni(III) complex **III**, reductive elimination furnishes the C–C coupled product and Ni(I) complex **IV**, which is then reduced *via* a single-electron transfer from the reduced-state photocatalyst, regenerating both the active Ni(0) complex **I** and the ground-state gCN, completing the catalytic cycle.

To confirm the presence of an alkyl radical species, we performed a radical trapping experiment (Scheme **5A**). Under our standard reaction conditions, the presence of TEMPO (2.5 equiv) completely shut down reactivity, resulting in no desired product. HRMS analysis of the reaction mixture confirmed the presence of the TEMPO-trapped benzylic radical **69**. Next, we performed a radical clock experiment with 2-cyclopropylacetic acid, a common carbon-based radical probe (Scheme **5B**). Using this as a substrate under our reaction conditions led to exclusive formation of the ring-opened product **70**, likely *via* rearrangement of the unstable cyclopropyl methyl radical intermediate, followed by subsequent nickel-mediated coupling. Finally, we monitored the reaction over time with varying concentrations of nickel catalyst, gCN photocatalyst, and varying light intensity (Scheme **5C**). Interestingly, varying the concentration of nickel had no discernible effect on the rate of product formation, with a similar reaction profile being observed with 2.5 mol %, 5 mol %, and 10 mol % nickel. Similarly, varying the amount of gCN used also had little effect on reaction rate – with product being generated at the same rate for 1.3, 2.5, and 5.0 mg mL^{-1} of photocatalyst. Finally, we measured the effect of the light intensity on reaction rate. In this case, the rate of product formation was clearly slowed down by the use of lower (25%) light intensity, suggesting that this reaction is operating in a photon-limited regime.

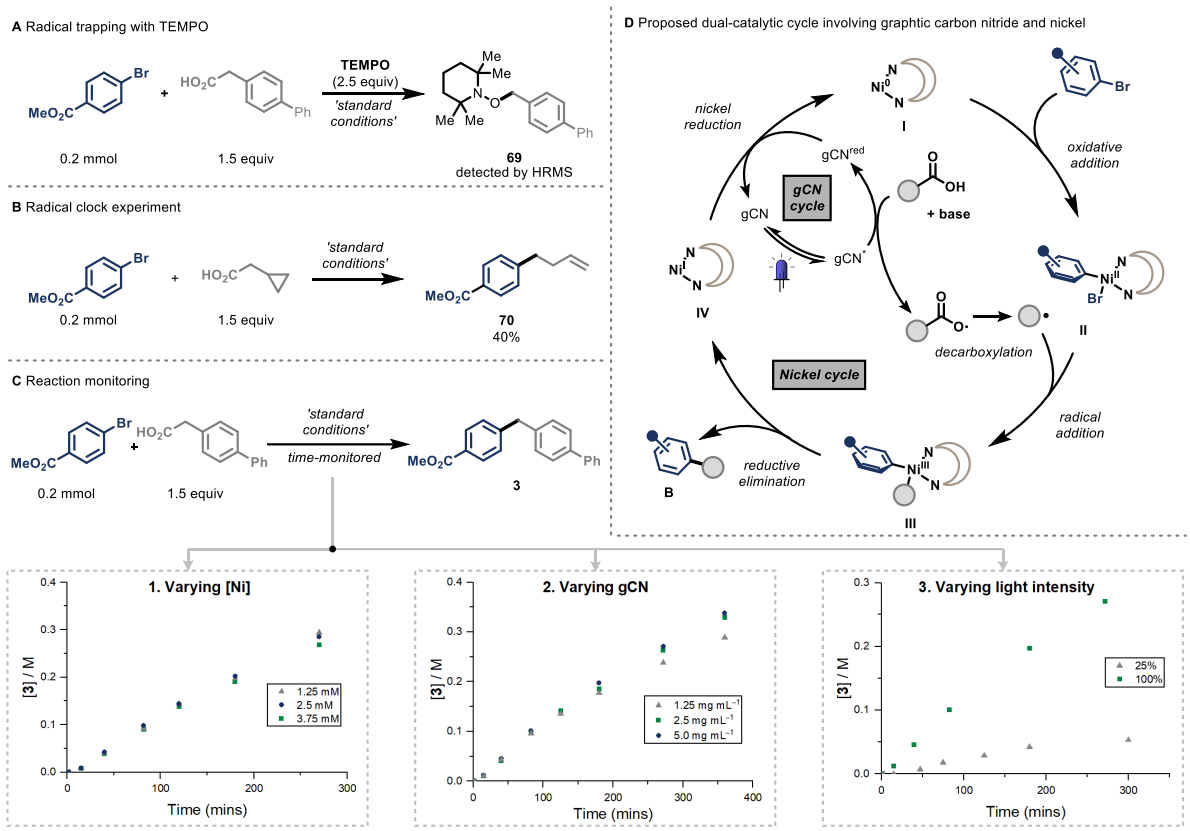

Scheme 5. (A) Radical trapping experiment, (B) Radical clock experiment, (C) Reaction monitoring for different [Ni], gCN loading, and light intensity, and (D) Plausible reaction mechanism.

CONCLUSION

In conclusion, we have successfully developed a C(sp^2)–C(sp^3) decarboxylative cross-coupling procedure, using abundant and commercially available aryl halide and alkyl carboxylic acid coupling partners. In contrast to previous procedures which utilise iridium, graphitic carbon nitride is demonstrated to be an effective alternative, facilitating the cross-coupling between a broad range of aryl halides and alkyl carboxylic acids. The environmental impact of graphitic carbon nitride has been assessed using the metric of Total Carbon Release, representing a clear improvement when compared with rare-earth metals. Finally, we have shown that the heterogeneous nature permits facile recovery of the photocatalyst post-reaction, which can be reused multiple times without a loss in reactivity. We envisage that heterogeneous semiconductor photocatalysts will continue to provide the cheap and abundant alternatives to traditional photocatalysts, and further studies are ongoing in our laboratories.

Author Contributions

MTF and FL designed the project, with input from TN and BM. MTF, FL, MF, and JT performed and analysed the synthetic experiments. Mechanistic studies, kinetic experiments and analytical measurements

were carried out by MTF and FL, and ES. All authors provided input during monthly update meetings. MTF, FL and TN wrote the manuscript with input from all authors.

Acknowledgements

The authors are grateful for generous funding from Novartis Pharma AG, from NWO (PhotoScale, NWO-OTP, No. 19887, TN and MF), and2 from the European Union H2020 under the ERC Consolidator Grant (FlowHAT, No. 101044355, TN and FL) and under the European Innovation Council project (reaCtor, No. 101099405, TN and ES).

References

(1) Biffis, A.; Centomo, P.; Del Zotto, A.; Zecca, M. Pd Metal Catalysts for Cross-Couplings and Related Reactions in the 21st Century: A Critical Review. *Chem. Rev.* **2018**, *118* (4), 2249–2295. https://doi.org/10.1021/acs.chemrev.7b00443.

(2) Wheelhouse, K. M. P.; Webster, R. L.; Beutner, G. L. Advances and Applications in Catalysis with Earth-Abundant Metals. *Org. Process Res. Dev.* **2023**, *27* (7), 1157–1159. https://doi.org/10.1021/acs.oprd.3c00207.

(3) Lipshutz, B.; Gallou, F.; Luescher, M. *The Impact of Earth-Abundant Metals as a Replacement for Pd in Cross Coupling Reactions*; preprint; Chemistry, 2024. https://doi.org/10.26434/chemrxiv-2024-tc9hm.

(4) Tasker, S. Z.; Standley, E. A.; Jamison, T. F. Recent Advances in Homogeneous Nickel Catalysis. *Nature* **2014**, *509* (7500), 299–309. https://doi.org/10.1038/nature13274.

(5) Ananikov, V. P. Nickel: The "Spirited Horse" of Transition Metal Catalysis. *ACS Catal.* **2015**, *5* (3), 1964–1971. https://doi.org/10.1021/acscatal.5b00072.

(6) Diccianni, J. B.; Diao, T. Mechanisms of Nickel-Catalyzed Cross-Coupling Reactions. *Trends Chem.* **2019**, *1* (9), 830–844. https://doi.org/10.1016/j.trechm.2019.08.004.

(7) Zuo, Z.; Ahneman, D. T.; Chu, L.; Terrett, J. A.; Doyle, A. G.; MacMillan, D. W. C. Merging Photoredox with Nickel Catalysis: Coupling of α-Carboxyl Sp ^{3} -Carbons with Aryl Halides. *Science* **2014**, *345* (6195), 437–440. https://doi.org/10.1126/science.1255525.

(8) Tellis, J. C.; Primer, D. N.; Molander, G. A. Single-Electron Transmetalation in Organoboron Cross-Coupling by Photoredox/Nickel Dual Catalysis. *Science* **2014**, *345* (6195), 433–436. https://doi.org/10.1126/science.1253647.

(9) Bonciolini, S.; Pulcinella, A.; Leone, M.; Schiroli, D.; Ruiz, A. L.; Sorato, A.; Dubois, M. A. J.; Gopalakrishnan, R.; Masson, G.; Della Ca', N.; Protti, S.; Fagnoni, M.; Zysman-Colman, E.; Johansson, M.; Noël, T. Metal-Free Photocatalytic Cross-Electrophile Coupling Enables C1 Homologation and Alkylation of Carboxylic Acids with Aldehydes. *Nat. Commun.* **2024**, *15* (1), 1509. https://doi.org/10.1038/s41467-024-45804-z.

(10) Luridiana, A.; Mazzarella, D.; Capaldo, L.; Rincón, J. A.; García-Losada, P.; Mateos, C.; Frederick, M. O.; Nuño, M.; Jan Buma, W.; Noël, T. The Merger of Benzophenone HAT Photocatalysis and Silyl Radical-Induced XAT Enables Both Nickel-Catalyzed Cross-Electrophile Coupling and 1,2-

Dicarbofunctionalization of Olefins. *ACS Catal.* **2022**, *12* (18), 11216–11225. https://doi.org/10.1021/acscatal.2c03805.

(11) *Native functionality in triple catalytic cross-coupling: sp3 C–H bonds as latent nucleophiles*. https://doi.org/10.1126/science.aaf6635.

(12) Gutiérrez-Bonet, Á.; Tellis, J. C.; Matsui, J. K.; Vara, B. A.; Molander, G. A. 1,4-Dihydropyridines as Alkyl Radical Precursors: Introducing the Aldehyde Feedstock to Nickel/Photoredox Dual Catalysis. *ACS Catal.* **2016**, *6* (12), 8004–8008. https://doi.org/10.1021/acscatal.6b02786.

(13) Knauber, T.; Chandrasekaran, R.; Tucker, J. W.; Chen, J. M.; Reese, M.; Rankic, D. A.; Sach, N.; Helal, C. Ru/Ni Dual Catalytic Desulfinative Photoredox Csp2–Csp3 Cross-Coupling of Alkyl Sulfinate Salts and Aryl Halides. *Org. Lett.* **2017**, *19* (24), 6566–6569. https://doi.org/10.1021/acs.orglett.7b03280.

(14) Corcé, V.; Chamoreau, L.-M.; Derat, E.; Goddard, J.-P.; Ollivier, C.; Fensterbank, L. Silicates as Latent Alkyl Radical Precursors: Visible-Light Photocatalytic Oxidation of Hypervalent Bis-Catecholato Silicon Compounds. *Angew. Chem. Int. Ed.* **2015**, *54* (39), 11414–11418. https://doi.org/10.1002/anie.201504963.

(15) Yoshida, J.; Nishiwaki, K. Redox Selective Reactions of Organo-Silicon and -Tin Compounds. *J. Chem. Soc. Dalton Trans.* **1998**, No. 16, 2589–2596. https://doi.org/10.1039/a803343i.

(16) Klauck, F. J. R.; James, M. J.; Glorius, F. Deaminative Strategy for the Visible-Light-Mediated Generation of Alkyl Radicals. *Angew. Chem. Int. Ed.* **2017**, *56* (40), 12336–12339. https://doi.org/10.1002/anie.201706896.

(17) Shu, C.; Noble, A.; Aggarwal, V. K. Photoredox-Catalyzed Cyclobutane Synthesis by a Deboronative Radical Addition–Polar Cyclization Cascade. *Angew. Chem. Int. Ed.* **2019**, *58* (12), 3870–3874. https://doi.org/10.1002/anie.201813917.

(18) Chan, A. Y.; Perry, I. B.; Bissonnette, N. B.; Buksh, B. F.; Edwards, G. A.; Frye, L. I.; Garry, O. L.; Lavagnino, M. N.; Li, B. X.; Liang, Y.; Mao, E.; Millet, A.; Oakley, J. V.; Reed, N. L.; Sakai, H. A.; Seath, C. P.; MacMillan, D. W. C. Metallaphotoredox: The Merger of Photoredox and Transition Metal Catalysis. *Chem. Rev.* **2022**, *122* (2), 1485–1542. https://doi.org/10.1021/acs.chemrev.1c00383.

(19) Gisbertz, S.; Pieber, B. Heterogeneous Photocatalysis in Organic Synthesis. *ChemPhotoChem* **2020**, *4* (7), 456–475. https://doi.org/10.1002/cptc.202000014.

(20) Chai, Z. Heterogeneous Photocatalytic Strategies for C(Sp^3)−H Activation. *Angew. Chem. Int. Ed.* **2024**, e202316444. https://doi.org/10.1002/anie.202316444.

(21) Savateev, O.; Zhuang, J. A Guide to Chemical Reactions Design in Carbon Nitride Photocatalysis. *ChemPhotoChem* **2024**, e202300306. https://doi.org/10.1002/cptc.202300306.

(22) Rocha, G. F. S. R.; Da Silva, M. A. R.; Rogolino, A.; Diab, G. A. A.; Noleto, L. F. G.; Antonietti, M.; Teixeira, I. F. Carbon Nitride Based Materials: More than Just a Support for Single-Atom Catalysis. *Chem. Soc. Rev.* **2023**, *52* (15), 4878–4932. https://doi.org/10.1039/D2CS00806H.

(23) Kumar, P.; Singh, G.; Guan, X.; Lee, J.; Bahadur, R.; Ramadass, K.; Kumar, P.; Kibria, Md. G.; Vidyasagar, D.; Yi, J.; Vinu, A. Multifunctional Carbon Nitride Nanoarchitectures for Catalysis. *Chem. Soc. Rev.* **2023**, *52* (21), 7602–7664. https://doi.org/10.1039/D3CS00213F.

(24) Singh, P. P.; Srivastava, V. Recent Advances in Visible-Light Graphitic Carbon Nitride ($g\text{-}C_3N_4$) Photocatalysts for Chemical Transformations. *RSC Adv.* **2022**, *12* (28), 18245–18265. https://doi.org/10.1039/D2RA01797K.

(25) Noël, T.; Zysman-Colman, E. The Promise and Pitfalls of Photocatalysis for Organic Synthesis. *Chem Catal.* **2022**, *2* (3), 468–476. https://doi.org/10.1016/j.checat.2021.12.015.

(26) Shi, J.; Yuan, T.; Zheng, M.; Wang, X. Metal-Free Heterogeneous Semiconductor for Visible-Light Photocatalytic Decarboxylation of Carboxylic Acids. *ACS Catal.* **2021**, *11* (5), 3040–3047. https://doi.org/10.1021/acscatal.0c05211.

(27) Wen, Z.; Wan, T.; Vijeta, A.; Casadevall, C.; Buglioni, L.; Reisner, E.; Noël, T. Photocatalytic C−H Azolation of Arenes Using Heterogeneous Carbon Nitride in Batch and Flow. *ChemSusChem* **2021**, *14* (23), 5265–5270. https://doi.org/10.1002/cssc.202101767.

(28) Shi, J.; Yuan, T.; Wang, R.; Zheng, M.; Wang, X. Boron Carbonitride Photocatalysts for Direct Decarboxylation: The Construction of C(Sp^3)–N or C(Sp^3)–C(Sp^2) Bonds with Visible Light. *Green Chem.* **2021**, *23* (11), 3945–3949. https://doi.org/10.1039/D1GC00922B.

(29) Murugesan, K.; Sagadevan, A.; Peng, L.; Savateev, O.; Rueping, M. Recyclable Mesoporous Graphitic Carbon Nitride Catalysts for the Sustainable Photoredox Catalyzed Synthesis of Carbonyl Compounds. *ACS Catal.* **2023**, *13* (20), 13414–13422. https://doi.org/10.1021/acscatal.3c03798.

(30) Khamrai, J.; Ghosh, I.; Savateev, A.; Antonietti, M.; König, B. Photo-Ni-Dual-Catalytic C(Sp^2)–C(Sp^3) Cross-Coupling Reactions with Mesoporous Graphitic Carbon Nitride as a Heterogeneous Organic Semiconductor Photocatalyst. *ACS Catal.* **2020**, *10* (6), 3526–3532. https://doi.org/10.1021/acscatal.9b05598.

(31) Bajada, M. A.; Di Liberto, G.; Tosoni, S.; Ruta, V.; Mino, L.; Allasia, N.; Sivo, A.; Pacchioni, G.; Vilé, G. Light-Driven C–O Coupling of Carboxylic Acids and Alkyl Halides over a Ni Single-Atom Catalyst. *Nat. Synth.* **2023**, *2* (11), 1092–1103. https://doi.org/10.1038/s44160-023-00341-3.

(32) Pieber, B.; Malik, J. A.; Cavedon, C.; Gisbertz, S.; Savateev, A.; Cruz, D.; Heil, T.; Zhang, G.; Seeberger, P. H. Semi-heterogeneous Dual Nickel/Photocatalysis Using Carbon Nitrides: Esterification of Carboxylic Acids with Aryl Halides. *Angew. Chem. Int. Ed.* **2019**, *58* (28), 9575–9580. https://doi.org/10.1002/anie.201902785.

(33) Beil, S. B.; Chen, T. Q.; Intermaggio, N. E.; MacMillan, D. W. C. Carboxylic Acids as Adaptive Functional Groups in Metallaphotoredox Catalysis. *Acc. Chem. Res.* **2022**, *55* (23), 3481–3494. https://doi.org/10.1021/acs.accounts.2c00607.

(34) Laudadio, G.; Palkowitz, M. D.; El-Hayek Ewing, T.; Baran, P. S. Decarboxylative Cross-Coupling: A Radical Tool in Medicinal Chemistry. *ACS Med. Chem. Lett.* **2022**, *13* (9), 1413–1420. https://doi.org/10.1021/acsmedchemlett.2c00286.

(35) Li, L.; Yao, Y.; Fu, N. Free Carboxylic Acids: The Trend of Radical Decarboxylative Functionalization. *Eur. J. Org. Chem.* **2023**, *26* (21), e202300166. https://doi.org/10.1002/ejoc.202300166.

(36) Prieto Kullmer, C. N.; Kautzky, J. A.; Krska, S. W.; Nowak, T.; Dreher, S. D.; MacMillan, D. W. C. Accelerating Reaction Generality and Mechanistic Insight through Additive Mapping. *Science* **2022**, *376* (6592), 532–539. https://doi.org/10.1126/science.abn1885.

(37) Lin, Y.; Malins, L. R. Total Synthesis of Biseokeaniamides A–C and Late-Stage Electrochemically-Enabled Peptide Analogue Synthesis. *Chem. Sci.* **2020**, *11* (39), 10752–10758. https://doi.org/10.1039/D0SC03701J.

(38) De Knaep, A. G. M.; Vandendriessche, A. M. J.; Daemen, D. J. E.; Dingenen, J. J.; Laenen, K. D.; Nijs, R. L.; Pauwels, F. L. J.; Van Den Heuvel, D. F.; Van Der Eycken, F. J.; Vanierschot, R. W. E.; Van Laar, G. M. L. W.; Verstappen, W. L. A.; Willemsens, B. L. A. Development Summary towards a

Manufacturable Process for R 83842 [(*S*)-6-[(4-Chlorophenyl) (1H-1,2,4-Triazol-1-Yl)Methyl]-1-Methyl-1H-Benzotriazole]. *Org. Process Res. Dev.* **2000**, *4* (3), 162–166. https://doi.org/10.1021/op990081n.

(39) Hou, Z.-W.; Liu, D.-J.; Xiong, P.; Lai, X.-L.; Song, J.; Xu, H.-C. Site-Selective Electrochemical Benzylic C−H Amination. *Angew. Chem. Int. Ed.* **2021**, *60* (6), 2943–2947. https://doi.org/10.1002/anie.202013478.

(40) gCN from three different commercially available sources were tested. Nanografi price 413 EUR/Kg (Correct as of 20/03/2024: https://nanografi.com/newly-released-products/graphitic-carbon-nitride-g-c3n4-powder-1-10-m/.

(41) Wen, Z.; Pintossi, D.; Nuño, M.; Noël, T. Membrane-Based TBADT Recovery as a Strategy to Increase the Sustainability of Continuous-Flow Photocatalytic HAT Transformations. *Nat. Commun.* **2022**, *13* (1), 6147. https://doi.org/10.1038/s41467-022-33821-9.

(42) Grimm, I.; Hauer, S. T.; Schulte, T.; Wycich, G.; Collins, K. D.; Lovis, K.; Candish, L. Upscaling Photoredox Cross-Coupling Reactions in Batch Using Immersion-Well Reactors. *Org. Process Res. Dev.* **2020**, *24* (6), 1185–1193. https://doi.org/10.1021/acs.oprd.0c00070.

(43) Onken, U.; Koettgen, A.; Scheidat, H.; Schueepp, P.; Gallou, F. Environmental Metrics to Drive a Cultural Change: Our Green Eco-Label. *CHIMIA* **2019**, *73* (9), 730. https://doi.org/10.2533/chimia.2019.730.

(44) Luescher, M. U.; Gallou, F. Interactions of Multiple Metrics and Environmental Indicators to Assess Processes, Detect Environmental Hotspots, and Guide Future Development. *Green Chem.* **2024**. https://doi.org/10.1039/D4GC00302K.